Facile construction of a molecularly imprinted polymer–based electrochemical sensor for the detection of milk amyloid A

Zhengrong Zhang[1] · Shisheng Chen[1] · Jianluan Ren[1] · Fang Han[2] · Xiaofeng Yu[2] · Fang Tang[1] · Feng Xue[1] · Wei Chen[3] · Jielin Yang[4] · Yuan Jiang[4] · Hongmei Jiang[1] · Bo Lv[1] · Jianguo Xu[3] · Jianjun Dai[1,5]

Abstract

A molecularly imprinted electrochemical sensor for the detection of serum amyloid A (MAA) in milk was established for early diagnosis of subclinical mastitis in dairy cows. The electrochemical sensor was initially constructed using a nanocomposite material (reduced graphene oxide/gold nanoparticles, AuNPs@rGO) to modify the working electrode. The template protein, MAA, was then immobilized using pyrrole as the functional monomer to carry out the electropolymerization. Finally, the template protein was removed to form a molecular imprint film with the capability to qualitatively and quantitatively signaling of MAA. Cyclic voltammetry (CV), differential pulse voltammetry (DPV), and scanning electron microscopy (SEM) were used to characterize the modification process of the molecularly imprinted electrochemical sensors. Under optimized conditions, the sensor shows two well-behaved linear relationships in the MAA concentration range 0.01 to 200 ng/mL. A lower detection limit was estimated to be 5 pg/mL (S/N = 3). Other parameters including the selectivity, reproducibility (RSD 3.2%), and recovery rate (96.1–103%) are all satisfactory. Compared with the traditional methods, detection of MAA to determine the subclinical mastitis of dairy cows can efficiently be diagnosed and hence prevent an outbreak of dairy cow mastitis. The electrochemical sensor can detect MAA more rapidly, sensitively, and inexpensively than the ELISA-based MAA detection. These advantages indicate that the method is promising for early diagnosis of dairy cows.

Keywords Subclinical mastitis · Milk amyloid A · Electrochemical sensor · Molecular imprinting · Nanocomposite

Introduction

Bovine mastitis affects the health of dairy cows and the profitability of herds worldwide, leading to a reduction in milk production and an increase in treatment costs. In severe cases, the lack of efficient interventions in the early stage of bovine mastitis causes huge economic losses to the breeding industry and dairy industry [1]. It can be divided into clinical mastitis (CM) and subclinical mastitis (SCM) types according to changes in milk and severity of inflammation. The incidence of SCM accounts for 77 to 79% of the total incidence. Due to the lack of obvious symptoms or local inflammation [2], SCM in cows is difficult to be found, resulting in increased milk production costs, reduced milk quality, increased treatment costs, and reduced farm income [3].

Subclinical mastitis is usually diagnosed by a bovine lateral examination such as the California Mastitis Test (CMT) [4] by laboratory analysis of somatic cell counting (SCC) or milk pathogen microbiological testing [5]. In some milking systems, conductivity can be used for on-line detection of mastitis

✉ Feng Xue
xuefeng@njau.edu.cn

✉ Jianguo Xu
Jgxu0816@163.com

1   MOE Joint International Research Laboratory of Animal Health and Food safety, Nanjing Agricultural University, Nanjing 210095, China

2   Hefei Customs Technical Center, Hefei 230601, China

3   Engineering Research Center of Bio-process, MOE, School of Biotechnology and Food Engineering, Hefei University of Technology, Hefei 23009, China

4   Technical Center of Animal Plant and Food Inspection and Quarantine, Shanghai Customs, Shanghai 200135, China

5   China Pharmaceutical University, Nanjing 211198, China

directly in milk [6]. However, these methods are less effective in detecting chronic subclinical mastitis cases than acute clinical cases [7]. Colorimetric and fluorometric methods have also been developed for measuring elevated enzyme concentrations (NAGase or LDH) in milk during mastitis [8]. However, the sensitivity is insufficient and the detection processes are affected by many factors. The milk pathogen microbial detection method is currently the "gold standard" for the detection of mastitis. The drawbacks of complicated, cumbersome, and time-intensive operations limit its application for the cases wherein fast detection is required. Accordingly, an urgent need exists to develop a fast, reliable, and simple new analytical method to detect and diagnose mastitis in dairy cows.

At present, the indicators of acute phase protein (APP), lactase, composition in milk, and blood routine indicators have become research hotspots in this regard [9]. APP is to stimulate the animal body to produce early proteins under the stimulation of stress, trauma, infection, or inflammation [10, 11]. Serum amyloid A (SAA) and haptoglobin (HP) are the two major APPs in cows [12]. Serum amyloid A is an APP with a variety of protein types, which is mainly induced by acute stimulation in the liver. Its main isoforms are SAA1, SAA2, and SAA3. SAA1 and SAA2 are mainly produced in the liver, while SAA3 is produced outside the liver and mainly found in milk [13]. Common detection methods for SAA include colloidal gold, enzyme-linked immunosorbent assay (ELISA), and latex enhanced immunoturbidimetric methods. The latex-enhanced immunoturbidimetric method is the most advanced, with a wider linear range and relatively simple procedures. The analytical sensitivity of the latex-enhanced immunoturbidimetric method is 3.52 mg/L. SAA3 in milk is called as milk amyloid A (MAA). Researches have revealed that during recessive mastitis in cows, the MAA content in milk of the cows increased significantly so that MAA has been identified as a sensitive indicator of cow mastitis infection [14–16]. According to reports, the only current method to detect MAA is the ELISA kits method [12, 17–19]. Although the ELISA method has high accuracy in detecting mastitis, it is time-consuming operations, high costs, non-specific results, and limited sensitivity.

As an promising alterative, the electrochemical sensor is a device that can utilize the electrochemical properties of the analyte and convert the chemical energy of interactions with the analyte into a recordable electrical signal, thereby realizing the analysis and detection of target analytes [20, 21]. When combined with molecularly imprinted technique, a method to produce molecularly imprinted polymers (MIP) that can accurately recognize a molecule, they show integrated favored features of easy operation, fast detection speed, low cost,

and high sensitivity and specificity [22, 23]. Molecularly imprinted electrochemical sensors (MIES) use a wholly synthetic recognition element which makes them less expensive devices than chemo/biosensors. MIESs display good devices with analytical capability towards small molecules and biomacromolecules [24, 25]. It has been widely used in the detection of various analytes, such as metal ions, small molecules, and proteins [26–28]. MIES fabrication involves immobilization of a molecularly imprinted polymer (MIP) onto the electrode surface, which is critical for high sensitivity. Because of the ultrahigh electron mobility of graphene and its unique structural property such as one-atom thickness and surface property like irreversible protein adsorption at the electrode surfaces, graphene-based materials might serve as an ideal platform for accommodating proteins and facilitating protein electron transfer [29]. AuNPs are used for several biomedical applications owing to their narrow size distribution, efficient surface modification, conductivity, attractive biocompatibility, and electrochemical properties [30].

Taken abovementioned into consideration, in this study, we constructed an excellent electrochemical sensor for MAA detection based on the employment of molecularly imprinting technique. A glassy carbon electrode was firstly modified with the nanocomposite material of reduced graphene oxide (rGO) and gold nanoparticles (AuNPs) (AuNPs@rGO). The material was prepared by loading rGO on AuNPs; resulting nanoparticles showed substantial electrical conductivity and biocompatibility [31]. MAA was subsequently used as the template molecule and electropolymerized using pyrrole as the functional monomer on the already modified electrode, ensuring the generated molecularly imprinted film with numerous and extremely specific recognition sites against the tested MAA. The successful establishment of this method is of great significance for early diagnosis of dairy cow mastitis.

Experimental

Reagents and materials

The rGO powders were obtained from Nanjing XFNANO Materials Tech. Co. Ltd. (Nanjing, China). Chloroauric acid ($HAuCl_4$), trisodium citrate ($\geq 99.9\%$), ethanol ($\geq 95\%$), potassium ferricyanide ($K_3[Fe(CN)_6]$), potassium ferrocyanide ($K_4[Fe(CN)_6]$), and KCl were purchased from Sinopharm Group Chemical Reagent Co. Ltd. (Shanghai, China). MAA was prepared and stored in this laboratory. Chitosan (chit, 99% deacetylation), glutaraldehyde (GA, 25% aqueous solution), casein (CS), bovine serum albumin (BSA), α-lactalbumin, and β-lactoglobulin were purchased from Sigma-Aldrich Chemical Co. (St. Louis, MO, USA). All chemicals were of analytical grade and used as received without further

purification. Hyper pure water (resistivity $=$ 18.2 MΩ cm^{-1}) was used throughout the experiment.

Cyclic voltammetry (CV) and differential pulse voltammetry (DPV) were performed on a CHI660D electrochemical workstation (Chenhua, Shanghai, China). In CV measurements, the range was performed from -0.1 to 0.6 V at a scan rate of 50 mV/s. In DPV measurements, the range was performed from -0.1 to 0.6 V at a scan rate of 50 mV/s with the pulse width, pulse period, and quiet time as 0.2 s, 0.5 s, and 2 s. The measurement was performed in a three-electrode cell that consists of a platinum wire auxiliary electrode, a saturated calomel reference electrode, and a bare or modified glassy carbon electrode (GCE, $\Phi = 3$ mm) (Chenhua, Shanghai, China) working electrode. All current tests were in PBS solution containing 10 mmol/L $[Fe(CN)_6]^{3-/4-}$ and 0.1 mol/L KCl. All measurements were carried out for 3 times at room temperature. Scanning electron microscope (SEM) and transmission electron microscope (TEM) characterization were performed on S8010 and H7650 (Hitachi, Japan), respectively. KQ 3200B ultrasonic cleaner from Kunshan Ultrasonic Instruments Co., Ltd. (China) was employed to clean electrodes.

Preparation of AuNPs@rGO nanocomposites

To prepare AuNPs, trisodium citrate dehydrate was used to reduce gold chloride (HAuCl$_4$) [32]. In brief, 50 mL ultrapure water was added to a clean triangle flask and heated on a magnetic stirrer until boiling. Then, 0.85 mL of 1% HAuCl$_4$ was quickly added to the triangle flask and 0.75 mL mass fraction of 1% trisodium citrate solution was added after a few seconds. The solution was heated for 10 min and then moved to an unheated plate for continued stirring. After

cooled to room temperature, the obtained AuNPs were stored at 4 °C and characterized by TEM.

To prepare AuNPs@rGO, the rGO (1 mg/mL) was thoroughly mixed with 0.25 mg/mL chitosan solution containing 0.02 mol/L acetic acid at a volume ratio of 1:1. Then, the equal volume of AuNP solution was added into the above mixture for ultrasonical mixing for 30 min to obtain AuNPs@rGO material [33] and adjust the final concentration of AuNPs@rGO dispersion to 1.0 mg/mL. The material compounding process was characterized by an ultraviolet-visible (UV-Vis) spectrophotometer.

Preparation of MIP-based electrochemical sensors

The preparation of the electrochemical sensor is shown in Fig. 1. Initially, the bare GCE was polished with an appropriate amount of Al$_2$O$_3$ with different particle sizes (1.0, 0.05, and 0.03 μm) to remove surface particles and ultrasonicated with ethanol and water. The electrode was then cleaned electrochemically in 0.1 M H$_2$SO$_4$ for 5 min with a scan rate of 50 mV/s, at potential range of -1.0 and 1.0 V for 50 cycles. After that, the three-electrode system was placed in PBS (pH 7.4) buffer containing 5 mmol/L [Fe (CN)6]$^{3-/4-}$ (1:1) and 0.1 mol/L KCl. CV was performed until a stable redox peak of $[Fe(CN)_6]^{3-/4-}$ appeared. Detailed sensor construction can be divided into six steps as follows:

(i)   Five microliters of AuNPs@rGO (1.0 mg/mL) nanocomposites was dropped onto the GCE surface and subsequently dried at room temperature

(ii) The modified electrode was activated with 5 μL of 2.5% GA (in PBS, pH 7.4) for 2 h and washed with water and dried at room temperature.

(iii) Five microliters of 100 μg/mL MAA was added to the electrode and reacted at room temperature for 1 h and then kept at 4 °C in refrigerator for 12 h. This was

Fig. 1 Scheme of the electrochemical sensor fabrication for MAA detection
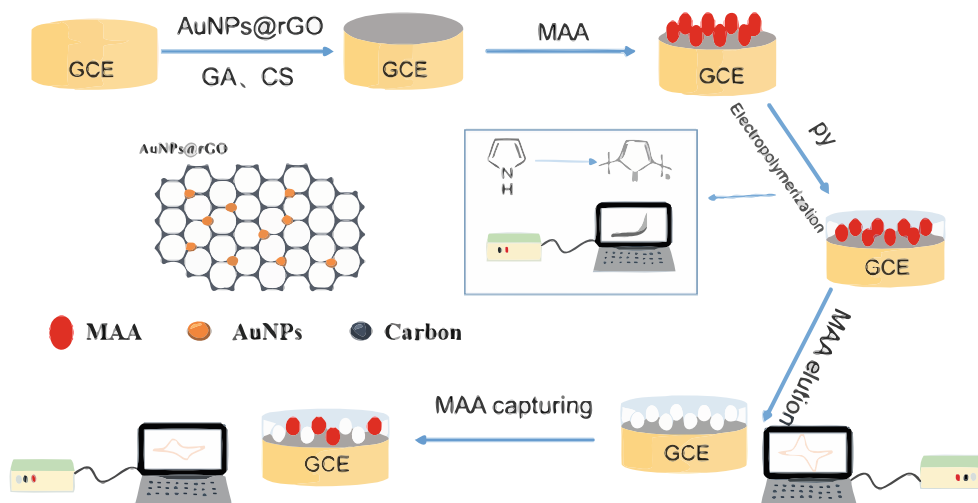
followed by washing the electrode with PBS (pH 7.4) to remove unbound MAA

(iv)   The MAA-modified electrode was immersed into 0.01 mol/L PBS (pH 7.4) solution containing 0.1 mol/L pyrrole, and electropolymerization was performed by scanning potential in the range of -0.3 to 0.8 V for 10 cycles with a scan rate of 50 mV/s. The solution had been continuously ventilated with nitrogen (N_2) for 30 min.

(v)   Removal of the template protein MAA was then conducted by immersing the polymer covered electrode into 2 mL of 10% (v/v) acetic acid solution containing 10% SDS for 1 h

(vi)   The final electrode was washed with PBS (pH 7.4) to obtain the molecularly imprinted electrode MIP/AuNPs@rGO/GCE that was conferred with target MAA recognition and signaling abilities. As a control, the non-imprinted polymer (NIP) modified GCE was fabricated following the same procedure, but in the absence of template molecules, and noted as NIP/AuNPs@rGO/GCE.

In order to examine the resorption performance of the sensor, both the MIP/AuNPs@rGO/GCE and NIP/AuNPs@rGO/GCE were immersed in a certain concentration

of MAA solution and incubated for 20 min. The current responses before washing, after washing, and after re-adsorption of MAA were tested.

Optimization of MAA sensor

The parameters for the fabrication and manipulation of MIP-based electrochemical sensor have great influences on the assay performance, such as sensitivity, selectivity, and reproducibility. In order to achieve the most effective combination of MAA, the conjugation conditions including the amount of AuNPs@rGO, the concentration of pyrrole, the number of electropolymerization scans, the electropolymerization rate, and the washing time and resorption time were investigated using single factor experiment.

Assay performance evaluation of MAA sensor

(i)   The MIP/AuNPs@rGO/GCE was immersed in different concentrations of MAA solution to investigate the linear relationship between the peak current difference ΔIp (between elution and resorption) and the MAA concentration and also the detection limit of the sensor.

(ii)   Other proteins such as casein (CS), bovine serum albumin (BSA), α-lactalbumin, and β-lactoglobulin with different molecular weights that may be present in milk

Fig. 2 TEM images of AuNPs before (a) and after optimization (b). The UV-Vis absorption spectrum of nanocomposites (c) ((a) rGO; (b) AuNPs; (c) AuNPs@rGO)
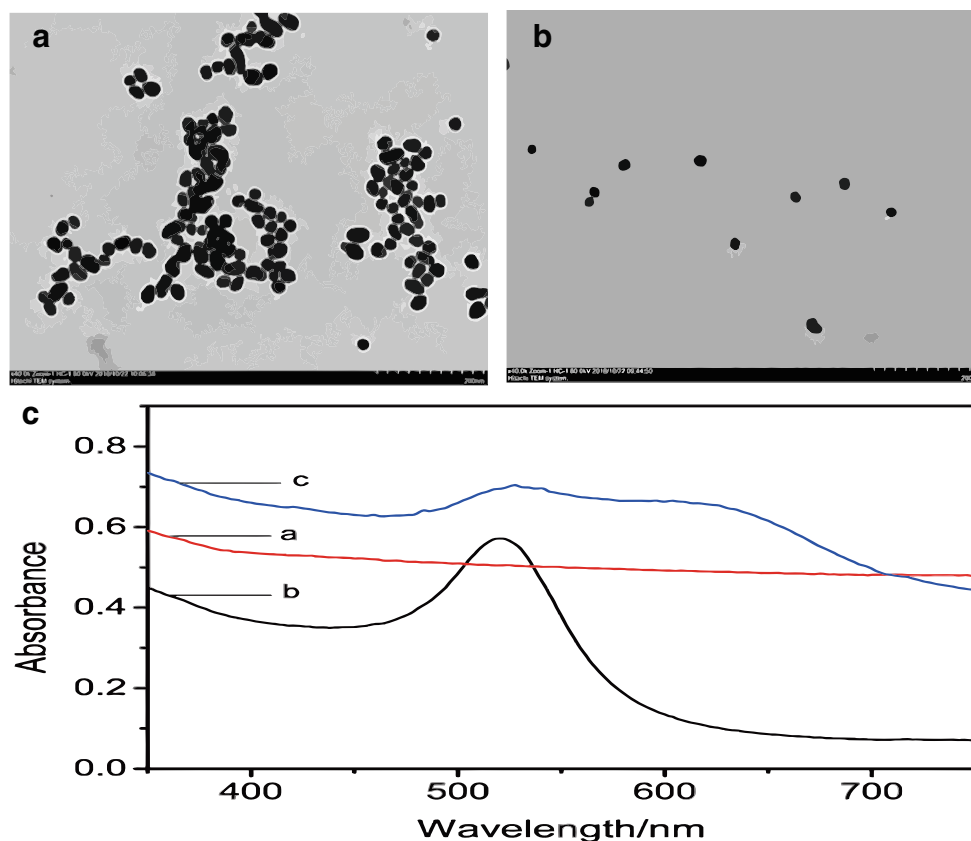
were selected as interfering substances. The sensor was used to simultaneously detect MAA and the above interfering proteins to evaluate the specificity of the sensor.

(iii) We have prepared five different MIP/AuNPs@rGO/GCEs under identical conditions and then tested them with the same concentration of MAA to evaluate the reproducibility of the sensor.

(iv) In order to evaluate the stability of the sensor, we put the prepared 5 electrodes (marked a, b, c, d, e) in a 4 °C refrigerator for 14 days. In the initial stage, the DPV current test was performed on the electrode every day, then every 2 days, and finally, the stability of the sensor was tested by observing the DPV signal change.

(v) In order to verify the practicability of the sensor, we have used a standard addition method to evaluate the sensor. The MAA standard was added to the fresh milk purchased on the market. We have first prepared the molecularly imprinted electrode according to the above method and then put the electrode into 0.5 mL of fresh milk with MAA concentration from 0.01 to 100 ng/mL. Depending on its DPV response, the detected concentration of MAA and the recovery rate of the sample were calculated. At the same time, we have compared the results with the

results of the purchased MAA ELISA kit (Tridelta Mast ID range MMA assay, Tridelta Development Ltd., Kildare, Ireland, Cat. No.: TP-807).

Results and discussion

TEM and UV-Vis characterization of nanomaterials

By optimizing the dosage of the reducing agent trisodium citrate, we obtained uniform AuNPs with better morphology and dispersion in Fig. 2b. The particle size is about 15 nm. Without optimization, the AuNPs are non-uniformly aggregated in Fig. 2a. From the UV characterization (Fig. 2c), we can see that the rGO (curve a) has no absorption peak in the wavelength range of 400–700 nm, AuNP shows an obvious characteristic absorption peak at around 520 nm (curve b), and AuNPs@rGO still displays a weak absorption at 520 nm. However, a wider absorption peak is seen over the range of 550–700 nm (curve c), indicating that a new characteristic absorption peak after rGO and AuNPs is combined. This absorption peak is significantly shifted to the right and is wider than the characteristic peak of AuNPs due to the

Fig. 3 SEM images of GCE (**a**), AuNPs@rGO/GCE (**b**), MIP/AuNPs@rGO/GCE with MAA (**c**), and MIP/AuNPs@rGO/GCE after elution (**d**)
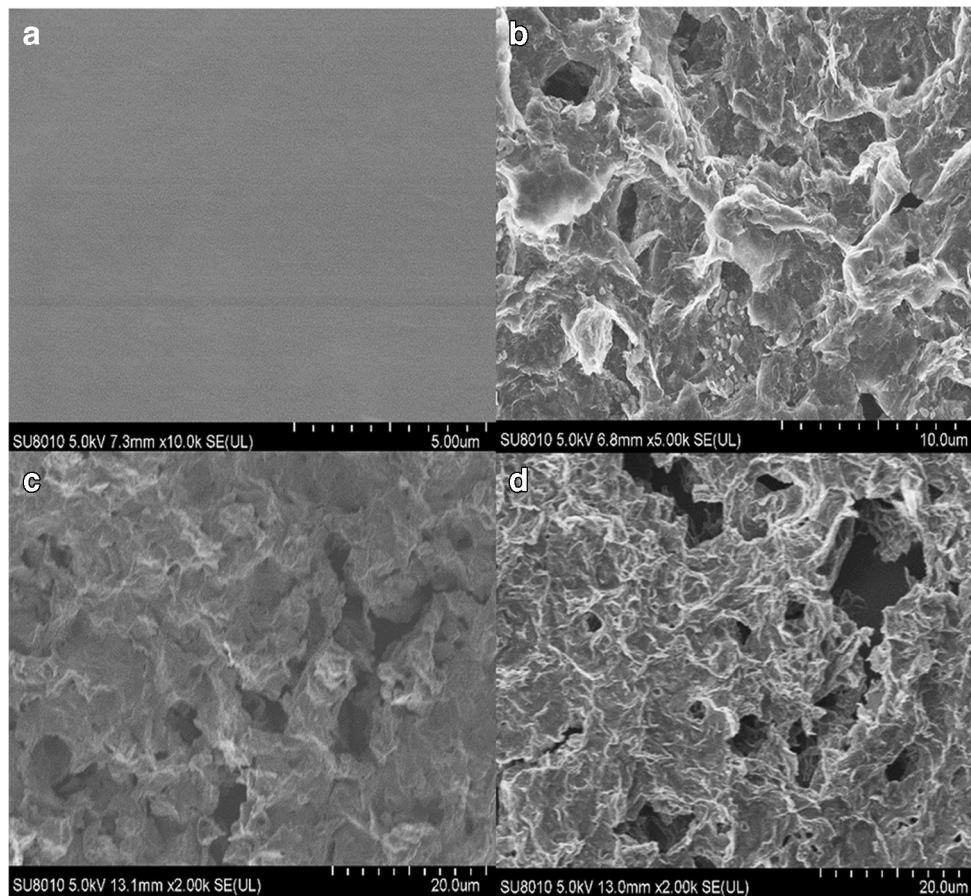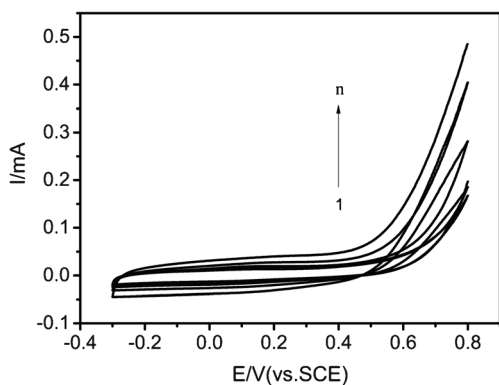
Fig. 4 CV image of the process of electropolymerization in 0.01 mol/L PBS (pH 7.4) solution containing 0.1 mol/L pyrrole

AuNPs@rGO broader particle size distribution and changes in particle structure.

SEM characterization of MIP/AuNPs@rGO/GCE

As shown in Fig. 3a, the surface of the bare GCE was smooth and non-grainy, indicating that the electrode has been completely polished. Figure 3 b shows the AuNPs@rGO

modified GCE, which is obviously different from Fig. 3a. It can be seen that AuNPs@rGO grows uniformly on the surface of the GCE. Figure 3 c shows the MIP/AuNPs@rGO/GCE before elution. At this time, the electrode surface was highly cross-linked to form a dense polypyrrole (ppy) film, indicating that the imprinted polymer was successfully prepared. In contrast, MIP/AuNPs@rGO/GCE in Fig. 3d was formed some imprinted cavities after removal of the MAA by the eluent, resulting in a rather rough surface than Fig. 3c.

Electrochemical behavior of the prepared MIP/AuNPs@rGO/GCE

Figure 4 shows the electropolymerization process on the electrode surface. It can be seen that during the whole electropolymerization process, the current response increased with the increasing of the number of scans. This phenomenon is ascribed to the gradual formation of electroactive polypyrrole on the electrode surface and in turn enhances the conductivity of the electrode.

CV and DPV were used to characterize the step-by-step modification process of bare GCE. Figure 5 a shows the CV curves of bare GCE (a), AuNPs@rGO/GCE (b), GA/
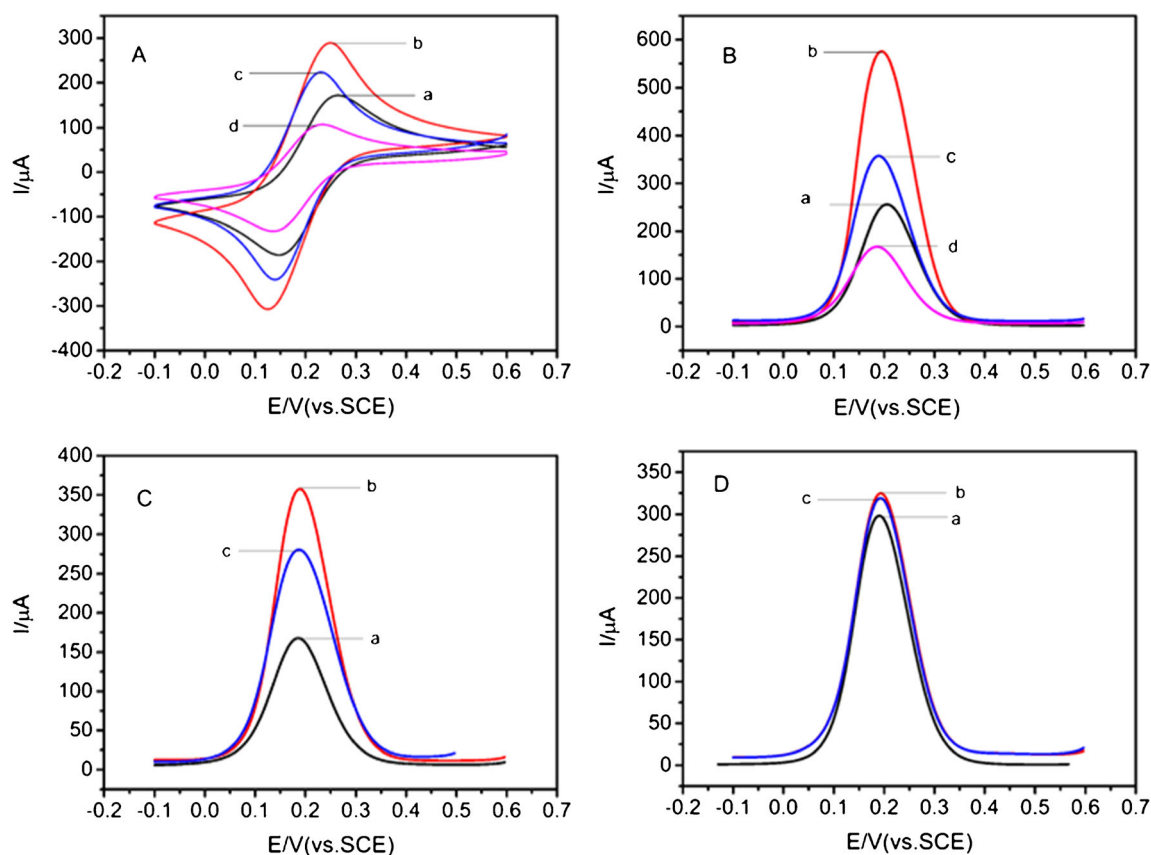

Fig. 5 The CV (**a**) and DPV (**b**) characterization of the stepwise modified electrodes((a) bare GCE; (b) AuNPs@rGO/GCE; (c) GA/AuNPs@rGO/GCE; (d) MAA/GA/AuNPs@rGO/GCE); DPV curves of MIP/AuNPs@rGO/GCE (**c**) and NIP/AuNPs@rGO/GCE (**d**): (a) before

removal of MAA from polymer; (b) after removal of MAA from polymer; (c) after incubating in 100 ng/mL MAA solution for 20 min in PBS (pH 7.4) containing 10 mmol/L [Fe(CN)$_6$]$^{3-/4-}$ (1:1) and 0.1 mol/L KCl

AuNPs@rGO/GCE (c), and MAA/GA/AuNPs@rGO/GCE (d) in 10 mmol/L of $[Fe(CN)_6]^{3-/4-}$ (1:1) and 0.1 mol/L of KCl solution, respectively. The bare GCE showed a pair of well-defined redox peaks (curve a). When the bare electrode was modified with AuNPs@rGO, the redox peak current increases significantly (curve b) due to the superior conductivity of the nanocomposite material. The subsequent cross-link of non-electroactive GA through its aldehyde group and the amino group of chitosan to form an imine bond led to an obvious decrease of the redox peak current (curve c). Similarly, the template molecule MAA attached to the electrode by GA based cross-linking caused a significant decrease of the redox peak current (curve d). This is because that the protein is a biomacromolecule with an insulation property, producing an obstructed electron transport layer on GA. As a result, these change tendencies demonstrate the successful step-by-step modification. Figure 5 b shows the DPV diagram of the electrode under the same modification conditions, which are overall consistent with the results in Fig. 5a, further proving the electrode modification.

DPV behaviors of both MIP/AuNPs@rGO/GCE and NIP/AuNPs@rGO/GCE are shown in Fig. 5 c and d. It can be clearly seen that even under the same conditions, they showed very big difference of current responses. In detail, the removal of template MAA (Fig. 5c, curve b) from the MIP/AuNPs@rGO/GCE electrode to form cavities resulted in a higher peak current than the raw MIP/AuNPs@rGO/GCE (Fig. 5c, curve a). This result shows that after removing the

template, the imprinting cavities created in the film can enhance the diffusion of $[Fe(CN)_6]^{3-/4-}$ to the sensor surface. After incubating the electrode with 100 ng/mL MAA for 30 min, the peak current was reduced (Fig. 5c, curve c). This indicates that the MAA is able to reoccupy the imprinting sites and block the free flow of electrons again. As a contrast, the same treatment of NIP/AuNPs@rGO/GCE electrode (Fig. 5d, curve a) with washing removal process (Fig. 5d, curve b) and re-incubation with MAA (Fig. 5d, curve c) can only induce slight differences. It means that no imprinted cavities are formed in the NIP in the absence of the MAA template.

Optimization of experimental conditions

Experimental optimization results are shown in Fig. 6. The peak current difference ΔIp before and after removal of MAA from polymer is selected as the investigation factor so that the larger the ΔIp is, the better the imprinting effect produces. Along this line, we have selected the optimal amount of AuNPs@rGO (1.0 mg/mL) to be 12 μL (Fig. 6a), the concentration of pyrrole is to be 80 mmol/L (Fig. 6b), the number of polymerization cycles is to be 10 (Fig. 6c), and the polymerization rate is to be 75 mV/s (Fig. 6d). In addition, by taking the peak current value Ip as the index for elution time and resorption time optimization, we have chosen the elution time of 25 min (Fig. 6e) and the resorption time of 20 min (Fig. 6f) as the best ones.
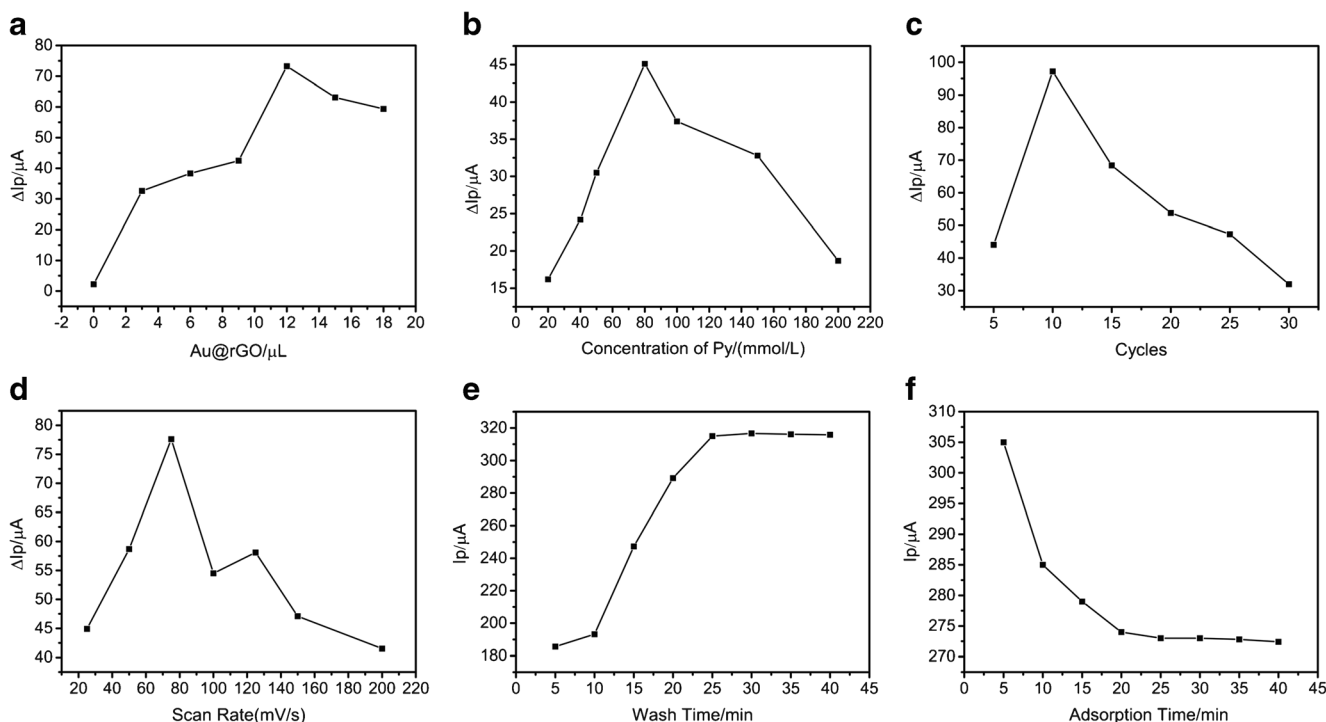

Fig. 6 Effects of **a** the amount of AuNPs, **b** the concentration of pyrrole, **c** electropolymerization scan cycles, **d** scan rate, **e** elution time, and **f** adsorption time on the assay performance. (All DPV tests are performed in PBS (pH 7.4) containing 10 mmol/L [Fe(CN)6]3−/4− (1:1) and 0.1 mol/L KCl.)
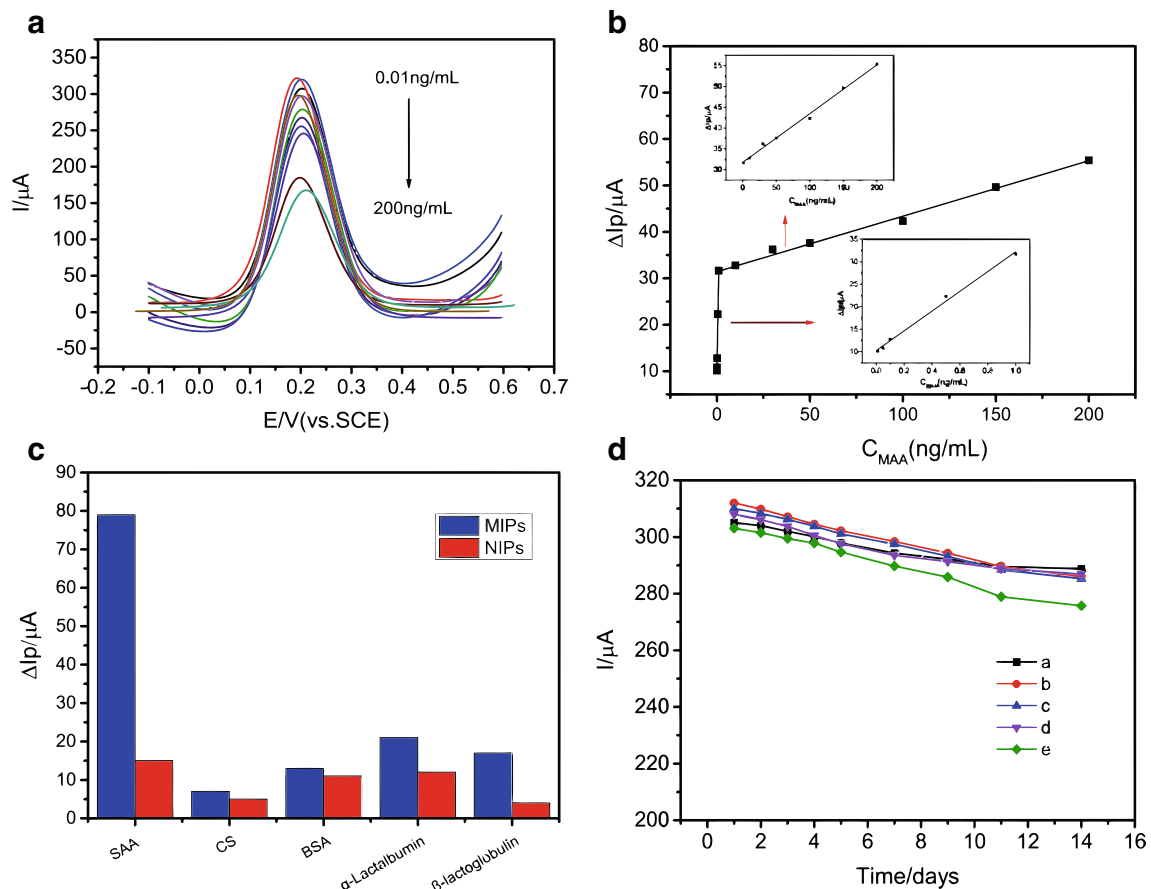
Fig. 7 DPV response of MIPs to different concentrations of MAA (**a**). The calibration plot of MIP/AuNPs@rGO/GCE electrode (**b**). The concentration of MAA ranges from 0.01 to 200 ng/mL, S/N = 3); selectivity of MIP- and NIP-based electrochemical sensors for MAA (**c**). Change of DPV responses within 2 weeks of five MIP-modified electrodes (**d**). (a, b, c, d, and e are the numbers of the electrodes which we tested)

Assay performance investigation and actual sample evaluation

Figure 7 a shows that the DPV current response of MIP/AuNPs@rGO/GCE is inversely proportional to the MAA concentration from 0.01 to 200 ng/mL. Interestingly, it is found in Fig. 7b that they are two linear relationships between the ΔIp

value and the target concentration. Achieved linear regression equations are ΔIp (μA) = 10.14 + 22.93 C_{MAA} (ng/mL) in the MAA concentration range 0.01–1 ng/mL ($R^2 = 0.991$), and ΔIp (μA) = 31.42 + 0.119 C_{MAA} (ng/mL) in the MAA concentration range 1 to 200 ng/mL ($R^2 = 0.994$), respectively. The slope of the regression equation at low target concentration is higher than the slope of the regression equation at high target concentration,

Table 1 Comparison of MAA detection in milk by this electrochemical sensor and ELISA kit

Sample	Added (ng mL^{-1})	Detected by this senor			Detected by ELISA		
		Found (ng mL^{-1})	Recovery (%)	RSD (%)	Found (ng mL^{-1})	Recovery (%)	RSD (%)
1	20	19.67	98.4	4.1	19.56	97.8	1.9
2	30	29.21	97.3	1.8	30.48	102	3.2
3	40	41.2	103	2.7	40.8	102	2.4
4	50	50.53	101	2.4	50.33	101	1.4
5	80	76.84	96.1	1.9	79.87	99.8	1.7
6	100	98.68	98.7	2.6	99.5	99.5	2.3

indicating that MAA molecularly imprinted electrochemical sensor has high and low affinity action points. When the concentration of MAA increases to a certain extent, the imprinting cavities are mostly occupied, resulting in a decrease in affinity. The LOD of the sensor is 5 pg/mL (S/N = 3). These results suggest that the MIP-based electrochemical sensor prepared has a wider detection range and a lower detection limit in comparison with ELISA.

The specific evaluation results are shown in Fig. 7c. The ΔIp response of MIP to MAA was at least 3 times higher than that of other interfering proteins, indicating a reasonable selectivity. Notably, the NIP-based electrochemical sensor does not give any response to target MAA or other interferents. Additionally, the relative standard deviation (RSD) of five different same-treated electrodes is about 2.2%, and the RSD value is about 3.2% for 5 times repeated determination, showing good reproducibility. Figure 7 d shows that the DPV signals of the five electrodes only show slight changes in 2 weeks, and the final peak value of the test current is 91–95% of the initial value. After 14 days, the five electrodes were immersed in 0.05, 0.1, 1, 50, and 100 ng/mL MAA solution for resorption testing. The RSD values of the test results were 3.6%, 4.1%, 2.4%, 1.9%, and 1.5%, indicating that the sensor has good stability.

The results of real sample determination are shown in Table 1. The obtained recoveries for MAA by the MIP-based electrochemical sensor in spiked milk are 96.1–103% with RSD values lower than 4.1%. The actual samples were also analyzed with ELISA method to trueness the efficiency of the developed technique. According to the kit instructions, a linear relationship between optical density at 450 nm(OD_{450nm}) and the MAA concentration was described by $OD_{450\ nm} = 0.0075 + 0.003\ C_{MAA}$ (ng/mL). The mimic MAA samples was prepared at the concentration of 20, 30, 40, 50, 80, and 100 ng/mL since the detection range of MAA in milk instructed by the commercial ELISA kit is 8.76–150 ng/mL. It can be seen from Table 1 that the detection performance of the sensor is not significantly different from the ELISA method. However, the sensor method is more advantageous in terms of ease of operation and time saving. It takes less than half an hour from incubation to detection and is simple to operate, while the ELISA takes 2–3 h with higher technical requirements.

Experimental results demonstrated that the MIP-based electrochemical sensor has excellent sensitivity, specificity, repeatability, stability, and applicability for MAA detection in a faster, cheaper, and simpler manner. These attributes suggest a substantial potential for use in the dairy industry. The biggest difficulty of this research is to ensure the repeatability of each operation. Electrochemical detection is very sensitive, and we must not introduce other impurities that affect the detection. Therefore, the electrode and container must be completely cleaned before each experiment. Also, the application of nanomaterials must be consistent, which requires technicians to be careful and rigorous.

Conclusions

In this study, based on molecularly imprinted electrochemical sensor technology, we have successfully prepared a sensor for the detection of MAA, the biomarker for subclinical mastitis in dairy cows. So far, there has been no report on the establishment of electrochemical detection method towards MAA in milk to monitor subclinical mastitis. Herein, we used a kind of "artificial receptor" by molecular imprinting to replace the traditional antibody, avoiding the cumbersome and expensive antibody preparation. Compared with conventional ELISA based detection method, it is simple and time-saving and has lower detection limit.

This study has important guiding significance for the study of acute-phase protein in dairy cows and the early diagnosis of subclinical mastitis, definitely providing new ideas for the detection of dairy cow mastitis. We expect that its application can greatly reduce farm economic losses caused by dairy cow mastitis. For long-term consideration, the sensor also has some limitations. If it is to be used in the clinic, further testing and analysis will be needed. Also, the application of this method to large-scale farm inspection is still difficult to achieve. Further optimization studies are needed to make this method more convenient and suitable for on-site testing.

Compliance with ethical standards

Conflict of interest The authors declare that they have no conflict of interest.

References

1. Heikkila AM, Nousiainen JI, Pyorala S (2012) Costs of clinical mastitis with special reference to premature culling. J Dairy Sci 95(1):139–150. https://doi.org/10.3168/jds.2011-4321

2. Akerstedt M, Waller KP, Sternesjo A (2009) Haptoglobin and serum amyloid a in bulk tank milk in relation to raw milk quality. J Dairy Res 76(4):483–489. https://doi.org/10.1017/S0022029909990185

3. Sender G, Pawlik A, Korwin-Kossakowska A (2017) Current concepts on the impact of coagulase-negative staphylococci causing bovine mastitis as a threat to human and animal health - a review. Anim Sci Paper Rep 35(2):123–135

4. Schalm OW, Noorlander DO (1957) Experiments and observations leading to development of the California mastitis test. J Am Vet Med Assoc 130(5):199–204

5. Schukken YH, Wilson DJ, Welcome F, Garrison-Tikofsky L, Gonzalez RN (2003) Monitoring udder health and milk quality using somatic cell counts. Vet Res 34(5):579–596. https://doi.org/10.1051/vetres:2003028

6. Zaninelli M, Tangorra FM, Costa A, Rossi L, Dell'Orto V, Savoini G (2016) Improved fuzzy logic system to evaluate Milk electrical conductivity signals from on-line sensors to monitor dairy goat mastitis. Sensors (Basel) 16(7). https://doi.org/10.3390/s16071079

7. Nielen M, Schukken YH, Brand A, Deluyker HA, Maatje K (1995) Detection of subclinical mastitis from online milking parlor data. J Dairy Sci 78(5):1039–1049. https://doi.org/10.3168/jds.S0022-0302(95)76720-0

8. Pyorala S (2003) Indicators of inflammation in the diagnosis of mastitis. Vet Res 34(5):565–578. https://doi.org/10.1051/vetres:2003026

9. Viguier C, Arora S, Gilmartin N, Welbeck K, O'Kennedy R (2009) Mastitis detection: current trends and future perspectives. Trends Biotechnol 27(8):486–493. https://doi.org/10.1016/j.tibtech.2009.05.004

10. Weng X, Ahmed SR, Neethirajan S (2018) A nanocomposite-based biosensor for bovine haptoglobin on a 3D paper-based analytical device. Sensor Actuat B-Chem 265:242–248. https://doi.org/10.1016/j.snb.2018.03.061

11. Lisowska-Myjak B, Skarzynska E, Plazinska M, Jakimiuk A (2018) Relationships between meconium concentrations of acute phase proteins. Clin Exp Pharmacol P 45(11):1218–1220. https://doi.org/10.1111/1440-1681.12995

12. Eckersall PD, Young FJ, Nolan AM, Knight CH, McComb C, Waterston MM, Hogarth CJ, Scott EM, Fitzpatrick JL (2006) Acute phase proteins in bovine milk in an experimental model of Staphylococcus aureus subclinical mastitis. J Dairy Sci 89(5):1488–1501. https://doi.org/10.3168/jds.S0022-0302(06)72216-0

13. McDonald TL, Larson MA, Mack DR, Weber A (2001) Elevated extrahepatic expression and secretion of mammary-associated serum amyloid a 3 (M-SAA3) into colostrum. Vet Immunol Immunopathol 83(3–4):203–211. https://doi.org/10.1016/s0165-2427(01)00380-4

14. Jaeger S, Virchow F, Torgerson PR, Bischoff M, Biner B, Hartnack S, Ruegg SR (2017) Test characteristics of milk amyloid a ELISA, somatic cell count, and bacteriological culture for detection of intramammary pathogens that cause subclinical mastitis. J Dairy Sci 100(9):7419–7426. https://doi.org/10.3168/jds.2016-12446

15. Domanska D, Gajewski Z, Domino M, Dazbrowski M, Kroemker V, Trela M (2015) Factors influencing serum amyloid a and Milk amyloid a concentrations in the predilection period of mastitis in mares. Reprod Domest Anim 50:51–51

16. Miglio A, Moscati L, Fruganti G, Pela M, Scoccia E, Valiani A, Maresca C (2013) Use of milk amyloid a in the diagnosis of subclinical mastitis in dairy ewes. J Dairy Res 80(4):496–502. https://doi.org/10.1017/S0022029913000484

17. Mcdonald TL, Weber A, Smith JW (1991) A monoclonal-antibody Sandwich immunoassay for serum amyloid-a (Saa) protein. J Immunol Methods 144(2):149–155. https://doi.org/10.1016/0022-1759(91)90081-P

18. Szczubial M, Dabrowski R, Kankofer M, Bochniarz M, Albera E (2008) Concentration of serum amyloid a and activity of ceruloplasmin in milk from cows with clinical and subclinical mastitis. B Vet I Pulawy 52(3):391–395

19. Thomas FC, Waterston M, Hastie P, Parkin T, Haining H, Eckersall PD (2015) The major acute phase proteins of bovine milk in a commercial dairy herd. BMC Vet Res 11:Artn 207. https://doi.org/10.1186/S12917-015-0533-3

20. Bakker E, Telting-Diaz M (2002) Electrochemical sensors. Anal Chem 74(12):2781–2800. https://doi.org/10.1021/ac0202278

21. Kan XW, Liu TT, Zhou H, Li C, Fang B (2010) Molecular imprinting polymer electrosensor based on gold nanoparticles for theophylline recognition and determination. Microchim Acta 171(3–4):423–429. https://doi.org/10.1007/s00604-010-0455-5

22. Nestora S, Merlier F, Beyazit S, Prost E, Duma L, Baril B, Greaves A, Haupt K, Tse Sum Bui B (2016) Plastic antibodies for cosmetics: molecularly imprinted polymers scavenge precursors of malodors. Angew Chem 55(21):6252–6256. https://doi.org/10.1002/anie.201602076

23. Attieh MD, Zhao Y, Elkak A, Falcimaigne-Cordin A, Haupt K (2017) Enzyme-initiated free-radical polymerization of molecularly imprinted polymer Nanogels on a solid phase with an immobilized radical source. Angew Chem Int Edit 56(12):3339–3343. https://doi.org/10.1002/anie.201612667

24. Jalalvand AR, Zangeneh MM, Jalili F, Soleimani S, Diaz-Cruz JM (2020) An elegant technology for ultrasensitive impedimetric and voltammetric determination of cholestanol based on a novel molecularly imprinted electrochemical sensor. Chem Phys Lipids 229:ARTN 104895. https://doi.org/10.1016/j.chemphyslip.2020.104895

25. Altintas Z, Gittens M, Guerreiro A, Thompson KA, Walker J, Piletsky S, Tothill LE (2015) Detection of waterborne viruses using high affinity molecularly imprinted polymers. Anal Chem 87(13):6801–6807. https://doi.org/10.1021/acs.analchem.5b00989

26. Whitcombe MJ, Chianella I, Larcombe L, Piletsky SA, Noble J, Porter R, Horgan A (2011) The rational development of molecularly imprinted polymer-based sensors for protein detection. Chem Soc Rev 40(3):1547–1571. https://doi.org/10.1039/c0cs00049c

27. Selvolini G, Marrazza G (2017) MIP-based sensors: promising new tools for cancer biomarker determination. Sensors-Basel 17(4):Artn 718. https://doi.org/10.3390/S17040718

28. Hansen DE (2007) Recent developments in the molecular imprinting of proteins. Biomaterials 28(29):4178–4191. https://doi.org/10.1016/j.biomaterials.2007.06.017

29. Gan T, Hu SS (2011) Electrochemical sensors based on graphene materials. Microchim Acta 175(1–2):1–19. https://doi.org/10.1007/s00604-011-0639-7

30. Rasheed PA, Sandhyarani N (2017) Electrochemical DNA sensors based on the use of gold nanoparticles: a review on recent developments. Microchim Acta 184(4):981–1000. https://doi.org/10.1007/s00604-017-2143-1

31. Wang X, Dong J, Ming H, Ai S (2013) Sensing of glycoprotein via a biomimetic sensor based on molecularly imprinted polymers and graphene-au nanoparticles. Analyst 138(4):1219–1225. https://doi.org/10.1039/c2an36297j

32. Mei ZL, Deng Y, Chu HQ, Xue F, Zhong YH, Wu JJ, Yang H, Wang ZC, Zheng L, Chen W (2013) Immunochromatographic